

1 **QTL mapping and identification of corresponding genomic regions for black pod disease resistance to three**  
2 ***Phytophthora* species in *Theobroma cacao* L.**

3  
4 Barreto MA<sup>1,2§</sup>, Rosa JRBF<sup>3§</sup>, Holanda ISA<sup>4#</sup>, Cardoso-Silva CB<sup>1</sup>, Vildoso CIA<sup>5</sup>, Ahnert D<sup>4</sup>, Souza MM<sup>4</sup>, Corrêa  
5 RX<sup>4</sup>, Royaert S<sup>6</sup>, Marelli J<sup>6</sup>, Santos ESL<sup>1,7</sup>, Luz EDMN<sup>2</sup>, Garcia AAF<sup>3</sup>, Souza AP<sup>1,8\*</sup>

6  
7 <sup>§</sup>*These authors contributed equally to this work*

8  
9 <sup>1</sup>Centro de Biologia Molecular e Engenharia Genética, Universidade Estadual de Campinas (UNICAMP),  
10 Campinas, SP, Brazil, CEP 13083-875

11 <sup>2</sup>Centro de Pesquisa, Assistência Técnica e Extensão Rural do Cacau, Comissão Executiva do Plano da Lavoura  
12 Cacaueira (CEPLAC), Ilhéus, Ba, Brazil, CEP 45600-970

13 <sup>3</sup>Departamento de Genética da Escola Superior de Agricultura “Luiz de Queiroz”, Universidade de São Paulo (USP),  
14 Piracicaba, SP, Brazil, CEP 13418-900

15 <sup>4</sup>Departamento de Ciências Biológicas, Universidade Estadual de Santa Cruz (UESC), Ilhéus, Ba, Brazil, CEP  
16 45662-900

17 <sup>5</sup>Instituto de Biodiversidade e Florestas, Universidade Federal do Oeste do Pará (UFOPA), Santarém, PA, Brazil,  
18 CEP 68035-110

19 <sup>6</sup>Mars Center for Cocoa Science (MCCS), Fazenda Almirante Rod. BR-101 km-484, Barro Preto, Ba,  
20 Brazil, CEP 45630-000

21 <sup>7</sup>Departamento de Ciências Exatas e Naturais, Universidade Estadual do Sudoeste da Bahia (UESB), Itapetinga, Ba,  
22 Brazil, CEP 45700-000

23 <sup>8</sup>Departamento de Biologia Vegetal, Instituto de Biologia, Universidade Estadual de Campinas (UNICAMP),  
24 Campinas, SP, Brazil, CEP 13083-862

25  
26 Corresponding author: Souza AP, phone: (+55) 19 35211132, fax: (+55) 19 35211089, e-mail: anete@unicamp.br

27  
28 **Abstract**

29 The cacao tree (*Theobroma cacao* L.) is a species of great importance because cacao beans are the raw material used  
30 in the production of chocolate. However, the economic success of cacao is largely limited by important diseases  
31 such as black pod, which is responsible for losses of up to 30-40% of the global cacao harvest. The discovery of  
32 resistance genes could extensively reduce these losses. Therefore, the aims of this study were to construct an  
33 integrated multipoint genetic map, align polymorphisms against the available cacao genome, and identify  
34 quantitative trait loci (QTLs) associated with resistance to black pod disease in cacao. The genetic map had a total  
35 length of 956.41 cM and included 186 simple sequence repeat (SSR) markers distributed among 10 linkage groups.  
36 The physical “*in silico*” map covered more than 200 Mb of the cacao genome. Based on the mixed model predicted  
37 means of *Phytophthora* evaluation, a total of 6 QTLs were detected for *Phytophthora palmivora* (1 QTL),  
38 *Phytophthora citrophthora* (1 QTL), and *Phytophthora capsici* (4 QTLs). Approximately 1.77% to 3.29% of the  
39 phenotypic variation could be explained by the mapped QTLs. Several SSR marker-flanking regions containing  
40 mapped QTLs were located in proximity to disease regions. The greatest number of resistance genes was detected in  
41 linkage group 6, which provides strong evidence for a QTL. This joint analysis involving multipoint and mixed-  
42 model approaches may provide a potentially promising technique for detecting genes resistant to black pod and  
43 could be very useful for future studies in cacao breeding.

44  
45 **Keywords:** Cacao, microsatellite markers, multipoint genetic map, composite interval mapping

## 46 Introduction

47 *Theobroma cacao* L. (also known as cacao or chocolate tree) is a perennial tree of the understory that  
48 belongs to the family Malvaceae. This tree is endemic to South American rainforests, which constitute a central  
49 region for the genetic diversity of these crops (Schultes and Cuatrecasas, 1964). *T. cacao* L. is a diploid species ( $2n$   
50  $= 2x = 20$ ) (Davie, 1935) with an estimated genome length of approximately 430 Mb (Argout *et al.*, 2011;  
51 Motamayor *et al.*, 2013). Cacao beans are the raw material used in the manufacturing of chocolate and cacao butter,  
52 because this, crops have become an economically important commodity for more than 50 tropical countries,  
53 generating approximately 12 billion dollars in revenue yearly (ICCO, 2014).

54 Black pod (also known as *Phytophthora* pod rot, PPR) causes serious economic problems in all cacao-  
55 growing regions worldwide (Lanaud *et al.*, 2009). This disease has affected cacao plantations since the 1920s and  
56 causes losses of up to 30-40% of the global production (Campêlo *et al.*, 1982; Tahi *et al.*, 2006). Black pod is caused  
57 by a complex of species belonging to the *Phytophthora* genus, which is known as the “plant destroyer” (Campêlo *et*  
58 *al.*, 1982). Currently, seven *Phytophthora* spp. have been reported in cacao disease etiology: *P. katsurae* Ko and  
59 Chang, *P. megakarya* Brasier and Griffin, *P. megasperma* Dreschler, *P. citrophthora* RE Smith and EH Smith, *P.*  
60 *heveae* Thompson, *P. capsici* Leonian, and *P. palmivora* (Butler) Butler (Luz *et al.*, 2004). Among these species, *P.*  
61 *palmivora* and *P. capsici* have a pantropical distribution, and both cause an estimated 20% to 30% annual loss and  
62 up to 10% of the tree deaths reported worldwide (Guest, 2007).

63 The symptoms and disease progression of black pod depend on the cacao genotype and the *Phytophthora*  
64 spp. involved; furthermore, they are influenced by climatic factors such as temperature, humidity and rainfall  
65 (Oliveira and Luz, 2005). Cacao pods are susceptible to fungal infection at all stages of development, and in the  
66 advanced stages of *Phytophthora* spp. infection, the beans become unsuitable for industrial use. Several measures  
67 have been used to control black pod disease, including appropriate cultural practices, fungicide application and the  
68 use of biological agents (*Trichoderma* spp.). However, these practices have substantial disadvantages, including  
69 increases in production costs, environmental pollution and ineffectiveness for field control (Nyassé *et al.*, 2003).  
70 Thus, genetic resistance is of great importance as a more effective, economical and sustainable alternative for black  
71 pod control, and molecular markers have emerged as important tools in the search for more effective solutions for  
72 genetic control (Michelmore, 2003).

73 QTL mapping has been proposed for different crop species and for many complex traits including disease  
74 resistance (Kover & Caicedo, 2001; Clair, 2010) using almost all of the current classes of molecular markers. In  
75 general, numerous disease-resistance QTLs have been detected in plants, as reviewed in detail by Kover & Caicedo  
76 (2001). These mapped QTLs were important for the investigation of genomic regions that potentially contain  
77 candidate genes for disease resistance. QTL mapping has been specifically developed for the cacao tree for the  
78 identification of QTLs associated with resistance to *Phytophthora* spp. (Crouzillat *et al.*, 2000a, b; Flament *et al.*,  
79 2001; Risterucci *et al.*, 2003; Clement *et al.*, 2003a; Lanaud *et al.*, 2004; Brown *et al.*, 2007).

80 However, none of the maps or linkage analyses published to date for cacao populations have been  
81 conducted using Wu’s multipoint approach (Wu *et al.*, 2002; Tong *et al.*, 2010). Unlike traditional two-point  
82 approaches, this procedure uses hidden Markov models (HMM) to estimate maximum likelihood based on the  
83 segregation patterns of all of the available markers in each linkage group, increasing the power to find the best  
84 ordering between them. The multipoint approach provides higher genetic information and increased saturation for  
85 the estimation of recombination fractions and linkage phases in map construction, which are conducted  
86 simultaneously in a full-sib population (Wu *et al.*, 2002). Consequently, the search for QTLs according to their  
87 positions and genetic effects is also achieved in a multipoint context (Gazaffi *et al.*, 2014), thereby increasing the  
88 power and confidence of the inferences.

89 Therefore, we propose that using a multipoint approach to construct the genetic linkage map will provide  
90 results with great power and confidence and enables conducting the QTL analyses for three *Phytophthora* species.  
91 The discovery of genomic regions containing resistance genes to black pod will be crucial for the inferring resistant  
92 phenotypes in future cycles of selection and for reducing the productivity losses resulting from this disease.

## 94 Materials and Methods

95 No specific permits were required for the described field studies. This work was a collaborative project  
96 developed by researchers from the MCCA (Brazil and USA), USP (Brazil), UNICAMP (Brazil), UESC (Brazil) and  
97 UFOPA (Brazil), UESB (Brazil), and CEPLAC (Brazil).

## 99 Plant Materials

100 The biological material used in the present study was obtained from the leaves of 265 individuals of an F1  
101 population (full-sib family) derived from a cross between the heterozygous clones TSH 1188 (Trinidad selected

102 hybrids; female parent) and CCN 51 (Colección Castro Naranjal; male parent). This population has been maintained  
103 in the MCCS located in Barro Preto, Bahia State, Brazil (14°42'45.021171" S and 39°22'13.008369" W). To obtain  
104 the F1 population, TSH 1188 and CCN 51 clones were maintained under controlled pollination according to the  
105 following procedure: the female flowers were protected for 24 h before pollination to avoid pollen contamination,  
106 and the cross was performed manually. The pods were collected and identified, the seeds were germinated, and the  
107 seedlings were planted in 3 × 3 m plots containing rows of 25 plants.

108 Both clones were selected because of their important contrasting agronomic traits, which include  
109 productivity, sexual incompatibility and disease resistance. Moreover, these clones are included in an international  
110 research program that is comprised of institutions from Brazil, Costa Rica and the United States. TSH 1188 was  
111 developed in Trinidad from the crosses of POUND 18 X TSH753 [open pollination X TSA 641 (SCA6 X IMC 67)]  
112 (ICGD, 2015), which produces rough red fruits, has self-incompatibility and is moderately resistant to black pod  
113 disease (Lopes *et al.*, 2011). CCN 51 was developed by H. Castro in the early 1960s in Ecuador from the following  
114 crosses: (ICS 95 X IMC 67) X Oriente 1 (Boza *et al.*, 2014); produces purplish-red immature fruits that become  
115 yellow-orange when ripe and have a slightly wrinkled rind, and the insides of the seeds have a clear purple color.  
116 This clone has been used as a parental genotype in many breeding and selection programs worldwide (Boza *et al.*,  
117 2014).

### 118 **Phenotypic Traits: Evaluation of Black Pod Disease**

119 Phenotypic evaluation of black pod disease in the F1 population was performed separately for the species  
120 *P. palmivora*, *P. citrophthora* and *P. capsici*, as described previously by Barreto *et al.* (2015). These three species  
121 were used because they are predominantly found in cacao production areas in Brazil. The *Phytophthora* isolates  
122 were obtained from laboratory culture collections (Phytolab) belonging to CEPLAC (Comissão Executiva do Plano  
123 da Lavoura Cacaueira). Zoospore suspensions for each *Phytophthora* species were obtained from cultures grown on  
124 Petri dishes containing carrot-water (*P. citrophthora*) or carrot-agar (*P. palmivora* and *P. capsici*) media for at least  
125 7 days (Supplementary Fig. 1).

126 Two 30-day inoculation series (trials) were conducted during the wet season for each *Phytophthora* species.  
127 In each inoculation series, 2-month-old leaves were collected early in the morning. Twenty discs from each  
128 individual were placed upside down on 8 plastic trays on 1-cm-thick dampened foam and incubated. Boxes  
129 containing a maximum of 48 cacao genotypes from the F1 population, parental clones TSH 1188 and CCN 51, and  
130 cultivars SCA 6 (resistant) and Catongo (susceptible) (Barreto *et al.*, 2015) were assembled into five different sets of  
131 individuals (boxes) that were replicated four times. Each individual was represented by five discs within each box.  
132 The boxes were distributed throughout a small laboratory area under controlled conditions, and the leaf discs were  
133 not exposed to any light source. Symptoms were observed 7 days after inoculation using the 6-point scale of  
134 infection (lesions) proposed by Nyassé *et al.* (1995), where 0 = no symptoms; 1 = very small localized penetration  
135 points; 2 = small penetration spots, sometimes in a network; 3 = coalescing lesions of intermediate size; 4 = large  
136 coalescing brown patches; and 5 = uniform large dark brown lesions.

137 Since the study by Nyassé *et al.* (1995) was published, the leaf-disc test applied in this study has been  
138 widely used to screen for resistance to black pod disease in cacao trees in studies conducted by Barreto *et al.* (2015)  
139 and Bahia *et al.* (2015). This analysis provides a rapid and early assessment of resistance levels, furthermore, a  
140 positive correlation between the data obtained by this method and the data obtained by field analyses has been  
141 observed, as well as anatomical similarities between the abaxial leaf side and the cacao pod epidermis (Nyassé *et al.*,  
142 1995; Tahi *et al.*, 2006; Santos *et al.*, 2009). In addition, Magalhães, *et al.* (2016) used this method to realize an  
143 indirect screening approach for *Ceratocystis* wilt resistance and found a positive correlation between the leaf disc  
144 method and field resistance.

145 The phenotypic data obtained for each *Phytophthora* species, based on the 6-point scale of infection  
146 (lesions), were analyzed according to the following statistical model:

$$147 y_{ijkl} = \mu + t_i + b_{j(i)} + g_k + d_{l(ijk)} + \epsilon_{ijk}$$

148 where  $y_{ijkl}$  corresponds to the level of black pod infection;  $\mu$  is the general average;  $t_i$  is the fixed effect of the  
149 inoculation series (trial)  $i$ ;  $b_{j(i)}$  is the fixed effect of box  $j$  nested within trial  $i$ ;  $g_k$  is the random effect associated with  
150 genotype  $k$ ;  $d_{l(ijk)}$  is the random effect associated with disc  $l$  nested within genotype  $k$ , box  $j$  and trial  $i$ ; and  $\epsilon_{ijk}$  is the  
151 random residual term among plots. The analyses were performed using GenStat software v.13 (Payne *et al.*, 2010)  
152 with a mixed-model approach (Henderson *et al.*, 1959; Robinson, 2012).

153 Different structures of variances and covariances were investigated for the genetic and residual matrices of  
154 the described mixed model. Briefly, we assessed models that could account for the heterogeneity of variances or the  
155 presence of covariances (correlations) between observations. We used the restricted maximum likelihood (REML)  
156 method (Patterson and Thompson, 1971) to estimate the random components of the models. The Akaike information  
157

158 criterion (AIC) (Akaike, 1974) was used to compare and select the best model. The fixed effects were analyzed  
159 using the Wald (test) statistics. The predicted means for the individuals were extracted from the most likely mixed  
160 model and used for QTL mapping.

161 In addition, estimates of genotypic and phenotypic variances as well as estimates of heritability and  
162 coefficients of variation were obtained from the analysis of each *Phytophthora* species. Moreover, genetic  
163 correlations between each pair of *Phytophthora* species were estimated from the predicted means using the Pearson  
164 coefficient, and a global level of 5% was considered statistically significant. The correlation analyses were  
165 performed using R software (R Development Core Team, 2014).

### 166 **DNA Extraction and Polymerase Chain Reaction (PCR) Amplification**

167 A modified *cetyltrimethylammonium bromide* (CTAB) method (Rehem *et al.*, 2010) was used to extract  
168 total genomic DNA from the leaves of each individual of the F1 population and from the parental clones TSH 1188  
169 and CCN 51. The DNA quality was evaluated on a 1% agarose gel and was compared with a standard lambda phage  
170 marker. The DNA quantity was estimated using a NanoDrop 8000 UV-VIS Spectrophotometer (Thermo Scientific,  
171 Brazil) at 260 nm.

172 Different SSR marker were available to genotype the F1 population, and the origin and institutions of these  
173 markers are described in Supplementary Table 1 (additionally, Appendix A and Appendix B present a detailed  
174 description of the loci). The PCR amplifications were performed in a Bio-Rad C1000TM Thermal Cyclers (Bio-Rad,  
175 USA) with a 15- $\mu$ L final volume containing 15 ng template DNA, 0.2  $\mu$ M each primer (forward and reverse), 100  
176  $\mu$ M each deoxynucleotide (dNTP), 2.0 mM MgCl<sub>2</sub>, 10 mM Tris-HCl, 50 mM KCl, 0.25  $\mu$ g  $\mu$ L<sup>-1</sup> bovine serum  
177 albumin (BSA) and 0.5 units of Taq DNA Polymerase (Invitrogen, SP, Brazil). The PCR program included an initial  
178 denaturation at 95°C for 5 min, followed by 30 cycles at the appropriate melting temperature (T<sub>m</sub>) for each primer  
179 for 1 min, 72°C for 1 min and 95°C for 1 min, with a final elongation step at 72°C for 30 min; the PCR  
180 amplification quality was evaluated on 3% agarose gels. Certain loci were subjected to electrophoresis on a 6%  
181 denaturing polyacrylamide gel in 1X Tris/Borate/EDTA (TBE) buffer, and a 10 bp ladder was used (Invitrogen, SP,  
182 Brazil) as a size standard. The DNA fragments were visualized using 0.2% silver-staining solution (Creste *et al.*,  
183 2001). Other loci were subjected to capillary electrophoresis in an ABI PRISM<sup>®</sup> 3100 Genetic Analyzer (Applied  
184 Biosystems), an automated system used for the analysis of fluorescently labeled DNA fragments. GeneMarker<sup>®</sup>  
185 software (SoftGenetics) was used to establish the peaks of filtering and interpretation, define the genotype of each  
186 individual, and generate the final compilation of data.

187 For each SSR marker, a classification (of 18 possible groups) was assigned to indicate the cross type and  
188 segregation (1:1:1:1, 1:2:1, 3:1, and 1:1) based on both parental and offspring marker band patterns, according to  
189 Table 1 proposed by Wu *et al.* (2002a).

### 190 **Genetic Linkage Map and Genome Alignment**

191 Marker segregation was assessed using a Chi-square test followed by the Bonferroni correction for multiple  
192 tests, according to the overall level of significance ( $\alpha = 5\%$ ). The integrated genetic linkage map was constructed  
193 using OneMap software v.2.0-3 (Margarido *et al.*, 2007) according to a multipoint approach based on the HMM  
194 (Wu *et al.*, 2002a; Wu *et al.*, 2002b). Initially, we obtained the pairwise linkage phases and recombination fractions  
195 between all the markers and separated these data into linkage groups (LGs) using a logarithm of the odds (LOD)  
196 score of 4.93 (an initial *empirical* threshold assigned based on the number of markers and Bonferroni correction)  
197 and a maximum recombination fraction of 0.30. Subsequently, the order of the markers within each LG was  
198 determined based on the HMM from a set of 5 initial markers, with the remaining markers subsequently added  
199 individually using the initial estimated order. The final multipoint recombination fractions between the markers were  
200 converted to centiMorgan (cM) units using the Kosambi mapping function (Kosambi, 1943). The final design of the  
201 map was generated using MapChart software v.2.2 (Voorrips, 2002).

202 The physical “*in silico*” map was constructed, which aligned the SSR marker sequences deposited in  
203 GenBank against the available cacao genome Criollo, using the nucleotide basic local alignment search tool  
204 (BLASTn) program. The cacao genome is available in the database *CocoaGen DB* (<http://cocoagendb.cirad.fr>),  
205 which has been developed and maintained by the Centre de Coopération Internationale en Recherche Agronomique  
206 pour le Développement (CIRAD) in France. An expected value (E-value) of 10 ( $e^{-10}$ ) was used to obtain an  
207 alignment with a lower probability of detecting false positives. An “*in silico*” PCR primer was used on the cacao  
208 genome v1.0 with an expected amplicon size between 40 to 1,000 bp, and a single mismatch was considered  
209 acceptable. The final design of the physical “*in silico*” map was also generated using MapChart software.

### 210 **QTL Mapping**

214 QTL analyses were performed using the multipoint genetic linkage map according to the model proposed  
215 by Gazaffi *et al.* (2014). This approach is an extension of the composite interval mapping (CIM) of Zeng (1993) for  
216 an outbred population. Initially, the entire genome was scanned to detect QTLs, and the conditional probabilities of  
217 the QTL genotypes were calculated every 1 cM based on a specific interval between two flanking markers. A  
218 maximum of 20 cofactors were included in the model to control for QTLs outside of the intervals. The markers used  
219 as cofactors were included based on the stepwise procedure and AIC (Akaike, 1974) for the selection of the final  
220 model. A window size of 15 cM was used to control the underlying information from both sides of each interval. To  
221 determine the presence of QTLs, LOD score-based thresholds were determined using 1,000 permutation tests  
222 (significance level of 0.95) based on the method of Chen and Storey (2006). The proportion of phenotypic variation  
223 ( $R^2$ ) explained by each QTL was calculated using least squares estimation.

224 Subsequently, genomic regions containing evidence of QTLs were fully investigated and tested for three  
225 possible effects according to Gazaffi *et al.* (2014): (i) additive for one parent, (ii) additive for the other parent, and  
226 (iii) dominance (intra-locus interactions between the additive effects of both parents). Based on the significance  
227 and signal of the QTL effects, the linkage phase between QTLs and flanking markers and QTL segregation at 1:1:1:1,  
228 1:2:1, 3:1 or 1:1 were inferred. Gazaffi's CIM extension was performed separately for each of the three  
229 *Phytophthora* species.

230

## 231 Results

232

### 233 Genetic Linkage Map

234 To evaluate polymorphisms in the F1 population, 83 SSR markers with polymorphic patterns in the  
235 parental clones TSH 1188 and CCN 51 were amplified. Fifty SSRs (60.24%) exhibited good amplification results.  
236 Of these, 30 SSRs (60.00%) were polymorphic in the F1 population, which allowed for the identification of 84  
237 different alleles. Other markers were also obtained from a database containing 199 SSRs from a group of various  
238 institutions involved in a cacao-breeding project – CIRAD, Universidade Estadual de Santa Cruz (UESC),  
239 Universidade Federal Rural do Semi-Árido (UFERSA) and MCCA. In total, 229 polymorphic SSRs were available  
240 for the construction of a genetic linkage map and for analyses of QTLs in the F1 population of the present study  
241 (Appendix A: mapped markers; Appendix B: unmapped/unlinked markers).

242 Of the 229 genotyped markers, 34 markers (14.85%) were heterozygous for TSH 1188, 48 markers  
243 (20.96%) were heterozygous for CCN 51, and 147 markers (64.19%) were heterozygous for both parents, exhibiting  
244 2 (34.70%), 3 (54.40%) or 4 (10.90%) alleles. Two hundred twenty-nine Chi-square tests, followed by Bonferroni  
245 correction, were performed for the polymorphic loci. The results revealed that 89 (out of 95 – 41.48%), 48 (out of 52  
246 – 22.71%) and 79 (out of 82 – 35.81%) loci exhibited an expected segregation of 1:1:1:1, 1:2:1 and 1:1,  
247 respectively. Thus, of the 229 markers, only 6 (2.62%), 4 (1.75%) and 3 (1.31%) markers showed significant  
248 deviations from the expected segregation of the respective classes, for a total of 13 (5.68%) deviated markers.  
249 However, because these markers did not show strong deviations of segregation, we used all of the information for  
250 the construction of a genetic linkage map. Three deviated markers (out of 13 – 23.08%) were incorporated into the  
251 final linkage map, and 10 (76.92%) remaining deviated markers were among the 42 (18.34%) SSRs that were not  
252 allocated into the map. Most of these unlinked markers presented a segregation of 1:1 (19; 45.24%), although a great  
253 proportion of segregation was also represented by 1:1:1:1 (16; 38.10%).

254 The multipoint genetic linkage map containing 186 SSRs is shown in Figure 1. Ten LGs were obtained  
255 from pairwise recombination fractions between the markers, which were considered linked when the estimated  
256 fractions were equal to or lower than 0.30 and when their LOD scores were equal to or higher than 4.93. We believe  
257 that the multipoint approach based on HMM provided accurate positioning of the markers and reliable distances  
258 from multipoint (upgraded) recombination fractions based on all of the available molecular information across each  
259 LG.

260 The total length of the multipoint linkage map is 956.41 cM (Table 1). Of the 10 identified LGs,  
261 corresponding to the haploid number of the cacao genome, six LGs exhibited larger genome coverage (in increasing  
262 order – LG 3, LG 4, LG 9, LG 2, LG 5 and LG 1). These LGs also had a higher number of markers (LG 3/LG 5, LG  
263 2, LG 9, LG 4 and LG 1), varying from 22 to 30, and generally had lower average distances between two adjacent  
264 markers (LG 4, LG 3, LG 1, LG 9, LG 2 and LG 5), exhibiting a high level of saturation of the cacao genome.

265

### 266 Genome Alignment: Physical “In Silico” Map

267 Recently, Argout *et al.* (2011) sequenced the genome of a suitable Belizean Criollo genotype (B97-61/B2),  
268 and these sequencing data are available in *CocoaGen DB*. The sequences of the 229 SSRs used in the present study  
269 were aligned against the B97-61/B2 genome. A physical “in silico” map was constructed from this alignment, and

270 217 SSRs were positioned to cover more than 200 Mb (202.74 Mb) of the cacao genome (Table 1; Figure 2). This  
271 coverage corresponds to 62.02% of the total available sequence (326.90 Mb), which covers 76.02% of the estimated  
272 genome of the B97-61/B2 genotype (430 Mb). Of the 10 chromosomes (Chrs) from the physical “*in silico*” map  
273 constructed in the present study, eight Chrs showed proportions above 50% (Chr 6, Chr 7, Chr 5, Chr 2, Chr 9, Chr  
274 3, Chr 4 and Chr 1) and three Chrs showed proportions above 70% (Chr 3 and Chr 1) of the B97-61/B2 genotype  
275 sequenced chromosomes (Table 1).

276 Of the 13 deviated markers from the F1 segregation patterns, 11 markers (84.62%) were allocated to the  
277 physical map. Moreover, this map positioned 38 SSRs that were not associated with any LGs of the multipoint  
278 genetic map (Figure 2). However, the multipoint genetic map of the present study accounted for 9 SSRs that were  
279 not aligned to any chromosomes of the physical map (Figure 1), demonstrating that both strategies were important  
280 for genome characterization. The distribution of the number of markers across the LGs and Chrs was similar  
281 between the linkage and physical maps (Table 1).

282

### 283 **Phenotypic Evaluation of Black Pod Disease**

284 A total of 265 individuals from the F1 segregating population, parental clones TSH 1188 and CCN 51, and  
285 cultivars SCA 6 (resistant) and Catongo (susceptible) were used to evaluate the responses to black pod infection  
286 caused by the three *Phytophthora* species. The parental clones and cultivars were used as references (checks) in the  
287 trials, allowing for the estimation of residual effects, and together with the F1 individuals, the investigation of  
288 genetic variances, covariances and correlations. The strategy used here was to test different structures of variances  
289 and covariances for the genetic-effects matrix grouping in the trials or boxes within each trial (Supplementary Table  
290 A).

291 For both *P. palmivora* and *P. capsici*, the models that better explained the genetic variation were compound  
292 symmetry heterogeneous ( $CS_{Het}$ ) for the trials and factor analytic of order 1 (FA) for the boxes within each trial. For  
293 *P. citrophthora*, the diagonal (DIAG) model was better adjusted for both trials and boxes within the trial. These  
294 results show that genetic variances between the trials and among the boxes within each trial were heterogeneous for  
295 the three *Phytophthora* species. However, genetic covariances and correlations were only detected for *P. palmivora*  
296 and *P. capsici* species, with an equal estimated correlation between the trials and different correlations among the  
297 boxes within each trial, varying according to the pairwise combination involving the boxes (Supplementary Table  
298 2).

299 The residual effects were also tested for complex models (results not shown). Convergence was not reached  
300 for these complex models based on the three *Phytophthora* species, which indicated that most of the variability  
301 likely reflected random genetic effects or that the adjustment of all the variance and covariance structures was too  
302 complex to reach convergence. The Wald test for fixed effects showed that only the boxes were significant (p-value  
303 < 0.001) for the three *Phytophthora* species (results not shown).

304 Comparative analyses between the black pod reactions of the inoculated parental clones (TSH 1188 and  
305 CCN 51) and cultivars (SCA 6 and Catongo) used as references revealed the efficiency of these cultivars as  
306 resistance and susceptibility standards, respectively (Supplementary Table 3). The parental clone CCN 51 showed  
307 high resistance to *P. palmivora* and moderate resistance to both *P. citrophthora* and *P. capsici*, whereas TSH 1188  
308 showed susceptibility to all species, when compared to the SCA 6 clone. The predicted mean of the F1 population  
309 was consistently higher than that of CCN 51 and SCA 6 and lower than that of TSH 1188 and Catongo. Phenotypic  
310 ( $\sigma_F^2$ ) and genotypic ( $\sigma_G^2$ ) variances were observed in the F1 population for all species. Higher genotypic variance was  
311 observed for *P. citrophthora* (1.164), followed by *P. palmivora* (1.151) and *P. capsici* (0.848). High heritability ( $h^2$ )  
312 was observed from the leaf-disc trials at 0.815 in *P. palmivora*, 0.903 in *P. citrophthora* and 0.639 in *P. capsici*. The  
313 coefficient of variation (CV %) varied from 6.757 to 8.511 (Supplementary Table A).

314 High and statistically significant Pearson correlation estimates were observed between *P. palmivora* and *P.*  
315 *citrophthora* ( $r = 0.730$ ; p-value = 0.000) and between *P. citrophthora* and *P. capsici* ( $r = 0.630$ ; p-value = 0.000),  
316 whereas a low and statistically significant Pearson correlation estimate was observed between *P. palmivora* and *P.*  
317 *capsici* ( $r = 0.340$ ; p-value =  $1.154 \times 10^{-8}$ ).

318

### 319 **QTL Mapping**

320 QTL mapping was performed based on the multipoint genetic map and predicted means of black pod  
321 disease from infections with *P. palmivora* (BP-Pp), *P. citrophthora* (BP-Pct) and *P. capsici* (BP-Pc). To identify  
322 QTLs, LOD score-based thresholds were obtained for the three *Phytophthora* species using 1,000 permutation tests,  
323 based on the method of Chen and Storey (2006), and produced the following values: 3.112 for BP-Pp, 3.058 for BP-  
324 Pct, and 3.174 for BP-Pc (Figure 3). A total of 6 QTLs were detected: 1 QTL for BP-Pp (LG 6), 1 QTL for BP-Pct  
325 (LG 6) and 4 QTLs for BP-Pc (LG 1, LG 2, LG 3 and LG 4) (Figure 3, Table 2, Supplementary Fig.2). Common

326 QTLs were not detected among the three *Phytophthora* species, although the Pearson correlation estimates were  
327 high and statistically significant between BP-Pp and BP-Pct and between BP-Pct and BP-Pc.

328 The proportion of phenotypic variation ( $R^2$ ) explained by the QTLs ranged from 1.77% to 3.29% (Table 2).  
329 The segregation patterns of the QTLs were 1:2:1 or 1:1. Of the 6 mapped QTLs, 5 QTLs (83.33%) had a significant  
330 additive effect for the parental clone TSH 1188 (i.e., with a LOD score higher than 0.834, that is the threshold with 1  
331 degree of freedom and 5% error probability), 1 QTL (16.66%) had a significant additive effect for the parental clone  
332 CCN 51, and 2 QTLs (33.33%) had a significant dominance effect from the interaction between both parents. Three  
333 QTLs (50.00%) had only an additive effect for the parental clone TSH 1188, whereas the other three QTLs showed  
334 at least two different effects that explained the phenotypic variation. QTLs with a significant additive effect were not  
335 exclusively observed for the parental clone CCN 51 (Table 2).

336 The QTL identified for *P. palmivora* (q1.BP-Pp) was located on LG 6 (73.00 cM) and explained 2.543% of  
337 the phenotypic variation (Table 2). This QTL showed a significant additive effect for the parental clone TSH 1188  
338 and had a segregation ratio of 1:1. The QTL identified for *P. citrophthora* (q1.BP-Pct) was also located on LG 6  
339 (0.00 cM) at position mTcCIR006 and explained 3.299% of the phenotypic variation. This QTL showed a  
340 significant dominance effect from the interaction between both parents and had a segregation ratio of 1:1. The 4  
341 QTLs identified for *P. capsici* explained 9.889% of the phenotypic variation. The first QTL (q1.BP-Pc) was located  
342 on LG 1 (117.00 cM) and showed either an additive effect for TSH 1188 or a dominance effect from the interaction  
343 between TSH 1188 and CCN 51. The second QTL (q2.BP-Pc) was located on LG 2 (81.00 cM), at position  
344 mTcCIR268, and showed two significant additive effects—one for each parent. The third QTL (q3.BP-Pc) was  
345 located on LG 3 (88.66 cM), at position mTcCIR202, and had a significant additive effect for TSH 1188. The fourth  
346 (and last) QTL (q4.BP-Pc) was located on LG 4 (22.00 cM) and had an additive effect for TSH 1188. These 4 QTLs  
347 for *P. capsici* explained 1.819%, 2.101%, 1.776% and 3.027% of the phenotypic variation and exhibited segregation  
348 ratios of 1:2:1 (q1.BP-Pc and q2.BP-Pc) or 1:1 (q3.BP-Pc and q4.BP-Pc).

349 The highest LOD score peaks of the mapped QTLs were observed for BP-Pc (Table 2). We identified peak  
350 LOD scores of 3.873, 3.643, 3.518 and 3.451 for q2.BP-Pc, q4.BP-Pc, q3.BP-Pc and q1.BP-Pc, respectively.  
351 However, although the LOD scores of the mapped QTLs for BP-Pp and BP-Pct were lower (3.228 for q1.BP-Pp and  
352 3.224 for q1.BP-Pct), the proportions of phenotypic variation were higher, with the exception of the QTL q1.BP-Pp  
353 ( $R^2 = 2.543$ ), when compared with the QTL q4.BP-Pc ( $R^2 = 3.027$ ).

### 354 **Co-localization of Disease Resistance-Related Genes and QTL Regions**

355 We further investigated the genes located close to the QTL regions associated with the three *Phytophthora*  
356 species using the chromosomal locations of the markers as a reference. These chromosomal locations were obtained  
357 from the first assembled *T. cacao* L. genome (Argout et al., 2011), which is available in the *CocoaGen DB*. Based  
358 on an average interval of 100 Kb for the six regions containing the mapped QTLs, we observed that most of the  
359 QTLs were located in genomic regions containing resistance-related genes (Appendix C).

## 360 **Discussion**

### 361 **Genetic Linkage Map**

362 The level of polymorphisms detected in the present study was expected based on previous cacao mapping  
363 studies (Flament et al., 2001; Risterucci et al., 2003; Allegre et al., 2012). The expected segregation ratios of most  
364 of the polymorphic loci indicated a favorable scenario for the construction of an integrated genetic map based on the  
365 multipoint approach. A total of 13 (5.68%) SSRs deviated from the expected segregation ratios based on the Chi-  
366 square tests and Bonferroni correction. However, these markers were not discarded for the construction of the  
367 genetic map because these distortions were not strong enough to cause potential problems. In the final genetic  
368 linkage map, three of these markers (mTcCIR035, mTcCIR099, and mTcCIR191) were positioned in three different  
369 LGs and helped to obtain a more precise representation of the cacao genome. In previously published genetic maps,  
370 approximately 11% of the markers exhibited a distortion of segregation (twofold of the proportion detected here)  
371 (Flament et al., 2001; Brown et al., 2007; Allegre et al., 2012). The origin of these distortions remains unknown but  
372 has been suggested to result from sub-lethal gametophytic selection, gamete-sporophytic incompatibility in the  
373 cacao gene systems or even structural changes, although the latter has never been reported in cacao studies (Fouet et  
374 al., 2011).

375 The cacao genetic linkage map constructed in the present study showed 10 LGs. The cacao tree is a diploid  
376 species with 20 chromosomes (Davie, 1935); therefore, this map represented the haploid number of cacao  
377 chromosomes (Figure 1). The marker distribution among the LGs was not uniform, and several gaps (approximately  
378 10 to 20 cM) were clearly observed in the multipoint genetic map, primarily in LGs 6, 7, 8 and 10, which has also

382 been described in previous genetic maps of cacao (Brown *et al.*, 2007; Allegre *et al.*, 2012). Of these LGs, saturation  
383 was lower for LG 10, as has also been described in other mapping studies (Brown *et al.*, 2007; Allegre *et al.*, 2012).  
384 One possible explanation for the gaps is that either the recombination events or the mapped loci were not evenly  
385 distributed for certain LGs (Souza *et al.*, 2013). These low-density markers might correspond to either highly  
386 homozygous regions that have a lower recombination frequency or centromeric regions.

387 The variation observed among cacao genetic linkage maps could partially reflect the use of different  
388 parental clones, progenies (F1, F2 or backcross), types and amounts of molecular markers, and algorithms to order  
389 and position the markers. We propose that the latter is crucial for obtaining more precise genetic linkage maps that  
390 may provide increased correspondence with the cacao genome. Our multipoint genetic map constructed from a cross  
391 between TSH 1188 and CCN 51 clones will be important for further studies on cacao breeding. These clones have  
392 contrasting agronomic traits associated with productivity and resistance to disease that are important traits for cacao  
393 breeding (with the SCA 6 clone serving as a standard resistance source).

### 394 **Physical “In Silico” Map**

395 The physical “in silico” map constructed here provides a rational guideline for cacao-breeding programs for  
396 the characterization of selected clones and germplasm collections using mapped SSRs, thus providing information  
397 for recurrent genome alignment studies, which can be difficult to obtain in certain scenarios. The high  
398 correspondence between linkage and physical maps (Supplementary Fig.3) clearly shows the power of the  
399 multipoint approach to construct genetic maps. In the present study, the physical map accounted for SSRs that were  
400 not present in any LGs of the genetic map, thus generating important additional information about the genome.  
401 However, the multipoint genetic map also accounted for SSRs that did not align to any chromosomes of the physical  
402 map, showing that both strategies are powerful and should be used whenever possible in genetic studies of cacao.

### 403 **Phenotypic Evaluation of Black Pod Disease**

404 Phenotypic analyses of black pod disease were performed using a mixed-model approach that allowed for  
405 the consideration of different scenarios for random genetic effects from the adjusted model, resulting in a model that  
406 can better explain experimental conditions and provide accurate predictions of the F1 individuals for QTL mapping.  
407 The findings of the present study suggest that more complex models provide more powerful explanations of the  
408 genetic variability of the *Phytophthora* species. The differentiated reaction of the cacao genotypes in response to  
409 *Phytophthora* spp. infection detected in this study was also observed in previous studies (Campêlo *et al.*, 1982).  
410 Campêlo *et al.* (1982) investigated the response of ‘comum’ variety cacao pods to *Phytophthora* species infection  
411 and reported that isolates of *P. citrophthora* showed higher virulence, whereas *P. palmivora* and *P. capsici* isolates  
412 showed intermediate and lower virulence, respectively. The mean values of the leaf lesions caused by *P.*  
413 *citrophthora* are approximately two times higher than the mean values of the leaf lesions caused by *P. palmivora* in  
414 clones TSH 1188 and CCN 51 (Bahia *et al.*, 2015). The moderate resistance of clone CCN 51 to *Phytophthora* spp.  
415 reflects the presence of genes potentially transferred from ICS 95 (Santos *et al.*, 2007), a moderately resistant clone  
416 that is an ancestor present in the CCN 51 genealogy. However, the low resistance to *Phytophthora* spp. presented by  
417 the clone TSH 1188 in this study was probably because the black pod isolates were more virulent, i.e. isolates 692  
418 (*P. capsici*), 1043 (*P. citrophthora*), and 2196 (*P. palmivora*), obtained from CEPEC *Phytophthora* collection. Our  
419 findings differ from the results showed by Bahia *et al.* (2015), who used the black pod isolates 62 (*P. citrophthora*)  
420 and 252 (*P. palmivora*).

421 The predicted mean of the F1 population was closer to the average of more resistant parental clones (i.e.,  
422 CCN 51 clone) for both *P. citrophthora* and *P. capsici*. The high estimates of heritability for the three *Phytophthora*  
423 species demonstrated that black pod disease in cacao may be controlled by a few genes and may be minimally  
424 influenced by the environment, suggesting a high magnitude for the correlation between phenotypic and genotypic  
425 values. Furthermore, the coefficients of variation for the three *Phytophthora* species were suitable, considering that  
426 the trials were performed under controlled conditions in a small laboratory area. Thus, the black pod trials were  
427 adequately conducted and were experimentally appropriate.

### 428 **QTL Mapping**

429 The present study is the first to use multipoint genetic linkage mapping (Wu *et al.*, 2002a, b; Margarido *et al.*,  
430 2007; Tong *et al.*, 2010), a mixed-model approach (Robinson, 2012) and CIM for an outbred population (Gazaffi  
431 *et al.*, 2014) for cacao genetic mapping. The results detected here could provide important insights that will increase  
432 our current understanding of the cacao genome and the genetic architecture of black pod disease. The six QTLs  
433 detected in this study were based on the LOD score thresholds obtained by permutation testing based on the method  
434 of Chen and Storey (2006) in that the present study considers different LOD score peaks to construct the statistical  
435  
436  
437



438 distribution and declare the level of significance; we believe that the use of this more relaxed significance criterion  
439 showed more acceptable results for detecting QTLs associated with black pod disease.

440 All of the QTLs detected here were mapped to different regions of the cacao genome. Thus, common QTLs  
441 were not observed among the three *Phytophthora* species, and these findings implicate important research directions  
442 that should be pursued. First, QTLs were observed in 5 (LG 1, LG 2, LG 3, LG 4 and LG 6) out of the 10 LGs  
443 constituting the cacao genome, showing that 50% of the genome included resistance-related genes to black pod.  
444 Second, the absence of common QTLs detected for the *Phytophthora* species suggested that their mechanisms of  
445 resistance could also be specific. This result is interesting because different mechanisms that utilize different  
446 resistance proteins and metabolic pathways could be specifically investigated and described. Moreover, this  
447 information could be useful for specific marker-assisted selection programs and cacao genetic-breeding programs,  
448 depending on the interest and purpose of the study.

449 The proportion of phenotypic variation ( $R^2$ ) explained by the QTLs detected here ranged from 1.77% to  
450 3.29% (Table 2). The QTL mapping of the present study was performed based on predicted means obtained from the  
451 mixed-model approach. Because the genetic effects were declared to be random in the mixed models, the predicted  
452 means were corrected by a *shrinkage* factor, which provides genetic effects that should be very close to the real  
453 values. Thus, we believe that the proportion of  $R^2$  explained by the QTLs in the present study was very reliable.  
454 Similar proportions of phenotypic variation have also been detected by other QTL studies that used mixed models  
455 for the phenotypic analyses in different plant species, such as the rubber tree (Souza *et al.*, 2013) and the common  
456 bean (Oblessuc *et al.*, 2014). However, a great proportion of phenotypic variation remains unexplained, assuming  
457 that the heritability of the black pod disease is high. One possible explanation is that the mapping population size  
458 used in the present study (265 F1 individuals) was not large enough to detect other possible QTLs with similar  
459 proportions of phenotypic variation compared with the mapped QTLs (Beavis, 1994; Bernardo, 2010). Another  
460 possible explanation is that interactions between the mapped QTLs and other possible QTLs (epistasis) may explain  
461 the high proportion of phenotypic variation. Epistasis effects should be important for black pod resistance because  
462 the molecular mechanisms of this disease seem to be very complex, as reported recently by Nyadanu *et al.* (2012).

463

#### 464 ***Co-localization of Disease Resistance-Related Genes and QTL Regions***

465 The mapped QTLs detected in the present study indicate genomic regions that should be further exploited  
466 to generate more polymorphisms for future studies of QTL mapping or to investigate resistance-related candidate  
467 genes. Flanking markers of the mapped QTLs were located in proximity to important genomic regions (Appendix  
468 C). An important predicted ortholog of leucine rich repeat (LRR)-containing receptors was located in the q2.BP-Pc  
469 and q4.BP-Pc regions; these receptors detect specific pathogenic peptides that signal to Pelle-family kinases (Dievert  
470 and Clark, 2004) and play central roles in signaling during pathogen recognition for the subsequent activation of  
471 defense mechanisms and developmental control (Afzal *et al.*, 2008). Two important genes encoding peroxidase 65  
472 and superoxide dismutase were mapped in the q2.BP-Cp region; peroxidase genes are involved in the response to  
473 environmental stresses, such as wounds and pathogen attacks (Kawano, 2003), whereas superoxide dismutase acts as  
474 an essential component in defense mechanisms against oxidative stress and pathogens (Bowler *et al.*, 1992). Genes  
475 assigned as Castor were identified in the q4.BP-Pc region; this gene is an ion channel that is likely involved in  
476 fungal entry into root epidermal cells during the establishment of mycorrhizal symbiosis (Charpentier *et al.*, 2008).  
477 Genes potentially involved in pathogen defense were identified in the q1.BP-Pp region, such as CPR30 that acts as a  
478 negative regulator of plant defense responses (Gou *et al.*, 2009), Cys5 that encodes a small protein with  
479 antimicrobial and antifungal activities that is expressed in various plant tissues (Lay and Anderson, 2005) and Y-3  
480 that interacts with the kinase domain under various experimental conditions, suggesting that Y-3 may be involved  
481 in stress conditions, such as mechanical wounding and pathogen infection (Tarutani and Sasaki, 2004). Moreover,  
482 we identified genes associated with the stress response and programmed cell death, such as BAG5 [101] and UPL5  
483 [102].

484

485

#### 486 ***Conclusion***

487 The number of genes involved in resistance to *Phytophthora* diseases is comparable to that observed in  
488 other species. Furthermore, the common regions of certain QTLs across different genetic groups confirm the  
489 existence of and potential use of these genes for marker-assisted selection programs. The identification of multiple  
490 QTLs involved in resistance to *Phytophthora* may be particularly useful when transferring different QTLs into an  
491 elite clone using a marker-assisted selection scheme. However, it would be interesting to evaluate interaction of  
492 these genes with other agronomic traits of interest to determine the relationship between resistance phenotypes in the  
493 field and yield components. We propose that a detailed functional genomics study should be performed to confirm

494 the roles of these QTLs associated with resistance to black pod disease. The multipoint genetic linkage and physical  
495 maps constructed in the present study will be useful for these further analyses.

496  
497

#### 498 **Acknowledgments**

499 The authors would like to thank the Comissão Nacional de Desenvolvimento Científico e Tecnológico (CNPq),  
500 Fundação de Amparo à Pesquisa do Estado da Bahia (FAPESB), Fundação de Amparo à Pesquisa do Estado de São  
501 Paulo (FAPESP, 2008/53197-4), Banco do Nordeste Brasileiro (BNB), Comissão Executiva do Plano da Lavoura  
502 Cacaueira (CEPLAC), Universidade Estadual de Campinas (UNICAMP), Universidade Estadual de Santa Cruz  
503 (UESC), and Coordenação de Aperfeiçoamento de Pessoal de Nível Superior (PROCAD-UESC, Computational  
504 Biology Program) for the grants provided for this research, FAPESP for the PhD fellowship to CBCS (2010/0354-2,  
505 2012/11109-0), and CNPq for the PhD fellowships to MAB, JRBFR and ESLS and for the research fellowships  
506 awarded to AAFG and APS. The authors would also like to thank the researchers from UNICAMP, UESC, MCCC  
507 and CEPLAC for supplying the physical structure required to perform this study. Additionally, the authors would  
508 like to thank Fernanda Bispo and Ademilde Cerqueira for assistance with black pod phenotyping, and Dr. Karina  
509 Gramacho for her invaluable help during the correction of the manuscript.

510  
511

#### 511 **Conflict of interest**

512 None of the authors have a conflict of interest to declare.

513

#### 514 **References**

515 Afzal AJ, Wood AJ, Lightfoot DA, 2008. Plant receptor-like serine threonine kinases: roles in signaling and plant  
516 defense. *Molecular Plant-Microbe Interactions* **21**, 507–17.

517 Akaike H, 1974. A new look at the statistical model identification. *IEEE Transactions on Automatic Control* **19**,  
518 716–23.

519

520 Allegre M, Argout X, Boccara M *et al.*, 2012. Discovery and mapping of a new expressed sequence tag-single  
521 nucleotide polymorphism and simple sequence repeat panel for large-scale genetic studies and breeding of  
522 *Theobroma cacao* L. *DNA Research* **19**, 23–35.

523

524 Argout X, Salse J, Aury J-M *et al.*, 2011. The genome of *Theobroma cacao*. *Nature Genetics* **43**, 101–8.

525 Bahia RDC, Aguilar-Vildoso CI, Luz EDMN, Lopes UV, Machado RCR, Corrêa RX, 2015. Resistance to black pod  
526 disease in a segregating cacao tree population. *Tropical Plant Pathology* **40**, 13–8.

527

528 Barreto MA, Santos JCS, Corrêa RX, Luz EDMN, Marelli J, Souza AP, 2015. Detection of genetic resistance to  
529 cocoa black pod disease caused by three *Phytophthora* species. *Euphytica* **206**, 677–87.

530

531 Bowler C, Montagu MV, Inze D, 1992. Superoxide dismutase and stress tolerance. *Annual Review of Plant*  
532 *Physiology and Plant Molecular Biology* **43**, 83–116.

533

534 Boza EJ, Motamayor JC, Amores FM *et al.*, 2014. Genetic characterization of the cacao cultivar CCN 51: its impact  
535 and significance on global cacao improvement and production. *Journal of the American Society for Horticultural*  
536 *Science* **139**, 219–29.

537

538 Brown JS, Phillips-Mora W, Power EJ *et al.*, 2007. Mapping QTLs for resistance to frosty pod and black pod  
539 diseases and horticultural traits in *Theobroma cacao*. *Crop Science* **47**, 1851–8.

540

541 Campêlo A, Luz E, Resnik F, 1982. Podridão parda do cacaueiro no Estado da Bahia, Brasil, 1: virulência das  
542 espécies de *Phytophthora*. *Revista Theobroma* **12**, 1–6.

543

544 Charpentier M, Bredemeier R, Wanner G, Takeda N, Schleiff E, Parniske M, 2008. *Lotus japonicus* CASTOR and  
545 POLLUX are ion channels essential for perinuclear calcium spiking in legume root endosymbiosis. *Plant Cell* **20**,  
546 3467–79.

547

548 Chen L, Storey JD, 2006. Relaxed significance criteria for linkage analysis. *Genetics* **173**, 2371–81.

549

- 550 Clair DA, 2010. Quantitative disease resistance and quantitative resistance loci in breeding. *Annual Review of*  
551 *Phytopathology* **48**, 247–68.
- 552
- 553 Clement D, Risterucci AM, Motamayor JC, N'goran J, Lanaud C, 2003. Mapping QTL for yield components, vigor,  
554 and resistance to *Phytophthora palmivora* in *Theobroma cacao* L. *Genome* **46**, 204–12.
- 555
- 556 Crouzillat D, Ménard B, Mora A, Phillips W, Pétiard V, 2000. Quantitative trait analysis in *Theobroma cacao* using  
557 molecular markers. *Euphytica* **114**, 13–23.
- 558
- 559 Davie JH, 1935. Chromosome studies in the malvaceae and certain related families. II. *Genetica* **17**, 487–98.
- 560 Flament MH, Kebe I, Clement D *et al.*, 2001. Genetic mapping of resistance factors to *Phytophthora palmivora* in  
561 cocoa. *Genome* **44**, 79–85.
- 562
- 563 Gazaffi R, Margarido GRA, Pastina MM, Mollinari M, Garcia AAF, 2014. A model for quantitative trait loci  
564 mapping, linkage phase, and segregation pattern estimation for a full-sib progeny. *Tree Genetics & Genomes* **10**,  
565 791–801.
- 566
- 567 Gou M, Su N, Zheng J *et al.*, 2009. An F-box gene, CPR30, functions as a negative regulator of the defense  
568 response in Arabidopsis. *Plant Journal* **60**, 757–70.
- 569
- 570 Guest D, 2007. Black pod: diverse pathogens with a global impact on cocoa yield. *Phytopathology* **97**, 1650–3.
- 571
- 572 Henderson CR, Kempthorne O, Searle SR, Von Krosigk C, 1959. The estimation of environmental and genetic  
573 trends from records subject to culling. *Biometrics* **15**, 192–218.
- 574
- 575 ICCO, 2014. Annual report. London United Kingdom 2013-2014. The International Cocoa Organization.  
576 [<http://www.icco.org/>]. Accessed 5 April 2014.
- 577 CGD, 2015. International Cocoa Germoplasm Database - CGD.  
578 [[http://www.icgd.rdg.ac.uk/ref\\_search.php?refcode=SHR96A](http://www.icgd.rdg.ac.uk/ref_search.php?refcode=SHR96A)]. Accessed 14 December 2016.
- 579
- 580 Kawano T, 2003. Roles of the reactive oxygen species-generating peroxidase reactions in plant defense and growth  
581 induction. *Plant Cell Reports* **21**, 829–37.
- 582
- 583 Kosambi DD, 1943. The estimation of map distances from recombination values. *Annals of Eugenics* **12**, 172–5.
- 584
- 585 Kover PX, Caicedo AL, 2001. The genetic architecture of disease resistance in plants and the maintenance of  
586 recombination by parasites. *Molecular Ecology* **10**, 1–16.
- 587
- 588 Lanaud C, Fouet O, Clément D *et al.*, 2009. A meta-QTL analysis of disease resistance traits of *Theobroma cacao*  
589 L. *Molecular Breeding* **24**, 361–74.
- 590
- 591 Lanaud C, Risterucci AM, Pieretti I, N'goran JaK, Fargeas D, 2004. Characterisation and genetic mapping of  
592 resistance and defence gene analogs in cocoa (*Theobroma cacao* L.). *Molecular Breeding* **13**, 211–27.
- 593
- 594 Lay FT, Anderson MA, 2005. Defensins-components of the innate immune system in plants. *Current Protein and*  
595 *Peptide Science* **6**, 85–101.
- 596
- 597 Lopes UV, Monteiro WR, Pires JL, Clement D, Yamada MM, Gramacho KP, 2011. Cacao breeding in Bahia, Brazil  
598 -strategies and results. *Crop Breeding and Applied Biotechnology* **1**, 73–81.
- 599
- 600 Luz EDMN, Sgrillo RB, Santosfilho LP, 2004. Estimativas de danos e perdas causadas por doenças no cacauero.  
601 In: *Proceedings of the Proceedings of the Workshop de Epidemiologia de doença*. Viçosa, 67–79.
- 602
- 603 Magalhães DMA, Luz EDMN, Lopes UV, Niella ARR, Damaceno VO, 2016. Leaf disc method for screening  
604 Ceratocystis wilt resistance in cacao. *Tropical Plant Pathology* **41**, 155–61.
- 605

- 606 Margarido GR, Souza AP, Garcia AA, 2007. OneMap: software for genetic mapping in outcrossing species.  
607 *Hereditas* **144**, 78–9.  
608
- 609 Michelmore RW, 2003. The impact zone: genomics and breeding for durable disease resistance. *Current Opinion in*  
610 *Plant Biololy* **6**, 397–404.  
611
- 612 Motamayor JC, Mockaitis K, Schmutz J *et al.*, 2013. The genome sequence of the most widely cultivated cacao type  
613 and its use to identify candidate genes regulating pod color. *Genome Biology* **14**, r53.  
614
- 615 Nyadanu D, Akromah R, Adomako B *et al.*, 2012. Biochemical mechanisms of resistance to black pod disease in  
616 cocoa (*Theobroma cacao* L.). *American Journal of Biochemistry and Molecular Biology* **3**, 20–37.  
617
- 618 Nyassé S, Cilas C, Herail C, Blaha G, 1995. Leaf inoculation as an early screening test for cocoa (*Theobroma cacao*  
619 L.) resistance to Phytophthora black pod disease. *Crop Protection* **14**, 657–63.  
620
- 621 Nyassé S, Mousseni IBE, Eskes AB, 2003. Selection for resistance to black pod disease and yield gains prediction  
622 by use of selected cocoa varieties in Cameroon. *Plant Genetic Resources* **1**, 157–60.  
623
- 624 Oblessuc PR, Baroni RM, Da Silva Pereira G *et al.*, 2014. Quantitative analysis of race-specific resistance to  
625 *Colletotrichum lindemuthianum* in common bean. *Molecular Breeding* **34**, 1313–29.  
626
- 627 Oliveira ML, Luz EDMN, 2005. *Identificação e Manejo das Principais Doenças do Cacau no Brasil*. Ilhéus:  
628 CEPLAC/CEPEC/SEFIT.  
629
- 630 Patterson HD, Thompson R, 1971. Recovery of inter-block information when block sizes are unequal. *Biometrika*  
631 **58**,  
632 545–54.  
633
- 634 Payne RW, Murray DA, Harding SA, Baird DB, Soutar DM, 2010. *GenStat for Windows, 13th Edn. Introduction*.  
635 Hemel Hempstead, UK: VSN International.  
636
- 637 Rehem BC, Almeida AA, Correa RX, Gesteira AS, Yamada MM, Valle RR, 2010. Genetic mapping of *Theobroma*  
638 *cacao* (Malvaceae) seedlings of the Parinari series, carriers of the lethal gene Luteus-Pa. *Genetics and Molecular*  
639 *Research* **9**, 1775–84.  
640
- 641 Risterucci AM, Paulin D, Ducamp M, N'goran JA, Lanaud C, 2003. Identification of QTLs related to cocoa  
642 resistance to three species of Phytophthora. *Theoretical and Applied Genetics* **108**, 168–74.  
643
- 644 Robinson GK, 2012. That BLUP is a good thing: the estimation of random effects. *Statistical Science* **6**, 15–32.  
645
- 646 Santos RMF, Lopes UV, Bahia RDC, Machado RCR, Ahnert D, Corrêa RX, 2007. Marcadores microssatélites  
647 relacionados com a resistência à vassoura-de-bruxa do cacau. *Pesquisa Agropecuária Brasileira* **42**, 1137–42.  
648
- 649 Santos ES *et al.*, 2009. Identifi cação de resistência genética do cacau à podridão-parda. *Pesq. agropec. bras.*,  
650 **44**(4), p.413–416.  
651
- 652 Schultes RE, Cuatrecasas J, 1964. Cacao and its allies. A taxonomic revision of the genus *Theobroma*. Review.  
653 *Economic Botany Journal* **19**, 416–7.  
654
- 655 Souza LM, Gazaffi R, Mantello CC *et al.*, 2013. QTL mapping of growth-related traits in a full-sib family of rubber  
656 tree (*Hevea brasiliensis*) evaluated in a sub-tropical climate. *PLoS One* **8**, e61238.  
657
- 658 Tahí GM, Kébé BI, Sangare A, Mondeil F, Cilas C, Eskes AB, 2006. Foliar resistance of cacao (*Theobroma cacao*)  
659 to *Phytophthora palmivora* as an indicator of pod resistance in the field: interaction of cacao genotype, leaf age and  
660 duration of incubation. *Plant Pathology* **55**, 776–82.  
661

- 662 Tarutani Y, Sasaki A, 2004. Identification of three clones which commonly interact with the kinase domains of  
663 highly homologous two receptor-like kinases, RLK902 and RKL1. *Bioscience, Biotechnology, and Biochemistry* **68**,  
664 2581–7.  
665
- 666 Tong C, Zhang B, Shi J, 2010. A hidden Markov model approach to multilocus linkage analysis in a full-sib family.  
667 *Tree Genetics & Genomes* **6**, 651–62.  
668
- 669 Voorrips RE, 2002. MapChart: software for the graphical presentation of linkage maps and QTLs. *Journal of*  
670 *Heredity* **93**, 77–8.  
671
- 672 Wu R, Ma CX, Painter I, Zeng ZB, 2002a. Simultaneous maximum likelihood estimation of linkage and linkage  
673 phases in outcrossing species. *Theoretical Population Biology* **61**, 349–63.  
674
- 675 Wu R, Ma C-X, Wu SS, Zeng Z-B (2002b) Linkage mapping of sex-specific differences. *Genet Res* 79:85–96. doi:  
676 10.1017/S0016672301005389.  
677  
678

679

## TABLES AND CAPTION (TITLE)

**Table 1.** Characterization of the linkage groups and chromosomes from the multipoint linkage and physical maps.

LG/Chr	Multipoint genetic linkage map (Figure 1)			Physical “ <i>in silico</i> ” map (Figure 2)			Proportion of the B97-61/B2 genome (%)
	Length (cM)	Number of markers	Average distance between markers (cM)	Length (Mb)	Number of markers	Average distance between markers (Mb)	
1	135.75	30	4.53	30.02	30	1.00	77.00
2	115.35	23	5.02	26.64	30	0.89	62.77
3	91.76	22	4.17	24.44	30	0.82	71.05
4	108.38	27	4.02	22.69	26	0.87	67.75
5	124.77	22	5.67	25.31	27	0.94	62.59
6	74.67	11	6.79	14.90	14	1.06	54.58
7	61.87	13	4.76	13.61	15	0.91	55.83
8	71.72	07	10.25	9.07	07	1.30	42.12
9	114.86	24	4.79	27.69	30	0.92	65.87
10	57.28	07	8.18	8.37	08	1.05	32.88
<b>Total</b>	<b>956.41</b>	<b>18.60</b>	<b>5.82</b>	<b>202.74</b>	<b>21.70</b>	<b>0.98</b>	<b>59.25</b>

680

**Table 2. Effects of QTLs mapped to black pod disease for an F1 segregating population.**

QTL	Flanking Markers	LG	Position in cM	Global LOD	$R^2$	$\alpha_{(TSH\ 1188)}$ (LOD)	$\alpha_{(CCN\ 51)}$ (LOD)	$\delta_{(TSH\ 1188,\ CCN\ 51)}$ (LOD)	Segregation
q1.BP-Pp	mTcCIR255 – mTcCIR009	6	73.00	3.228	2.543	0.213 (2.485)	- 0.080 (0.384)	- 0.096 (0.507)	1:1
q1.BP-Pc	mTcCIR273 – mTcCIR275	1	117.00	3.451	1.819	0.251 (0.897)	- 0.209 (0.643)	0.179 (1.925)	1:2:1
q2.BP-Pc	mTcCIR268	2	81.00	3.873	2.101	0.179 (2.193)	0.247 (1.767)	0.004 (0.001)	1:2:1
q3.BP-Pc	mTcCIR202	3	88.66	3.518	1.776	- 0.218 (2.513)	0.080 (0.511)	- 0.074 (0.405)	1:1
q4.BP-Pc	mTcCIR237 – mTcCIR095	4	22.00	3.643	3.027	0.502 (3.609)	- 0.006 (0.002)	0.014 (0.015)	1:1
q1.BP-Pct	mTcCIR006	6	0.00	3.224	3.299	0.089 (0.481)	- 0.091 (0.520)	0.173 (1.823)	1:1

LG indicates the linkage group where the QTL was detected.

$R^2$  is the proportion of phenotypic variation explained by the QTL.

The global LOD values were compared with the LOD score thresholds calculated using 1,000 permutation tests based on the methods of (i) [85] and (ii) [86], and the respective values were 4.004 and 3.112 for *P. palmivora*, 4.165 and 3.058 for *P. citrophthora*, and 4.167 and 3.174 for *P. capsici*.

$\alpha_{(TSH\ 1188)}$  is the estimated additive effect for the parental clone TSH 1188,  $\alpha_{(CCN\ 51)}$  is the estimated additive effect for the parental clone CCN 51, and  $\delta_{(TSH\ 1188,\ CCN\ 51)}$  is the estimated dominance effect from the interaction between both parents TSH 1188 and CCN 51. The LOD scores of the regions with evidence of QTLs were compared with LOD = 0.834 (Chi-square distribution, with 1 degree of freedom and 5% error probability).

682  
683  
684  
685  
686  
687  
688  
689  
690  
691  
692  
693  
694  
695  
696  
697  
698  
699  
700  
701  
702  
703  
704  
705

## FIGURE CAPTIONS

**Figure 1. Multipoint integrated genetic linkage map constructed for the cacao tree (*Theobroma cacao* L.) using 265 individuals of an F1 segregating population (TSH 1188 X CCN 51).**

This map consists of 186 SSRs covering a total of 956.41 cM. The asterisks shown at the end of the name of some markers represent the following: \*, deviation of segregation (ds); \*\*, not aligned in the physical “*in silico*” map; \*\*\*, not aligned in the same group/chromosome of the physical map; \*\*\*\*, (ds) and not aligned in the physical map; and \*\*\*\*\*, (ds) and not aligned in the same group/chromosome of the physical map.

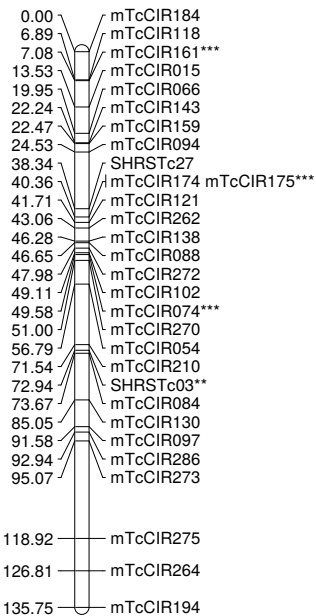
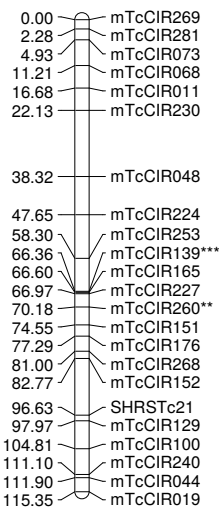
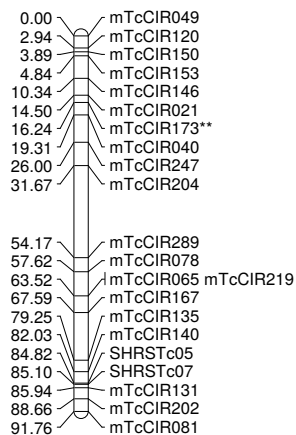
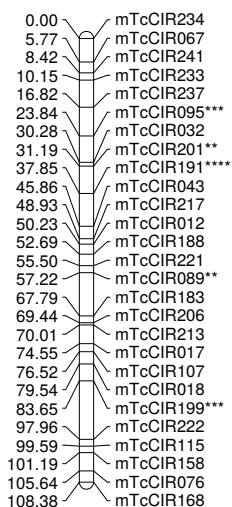
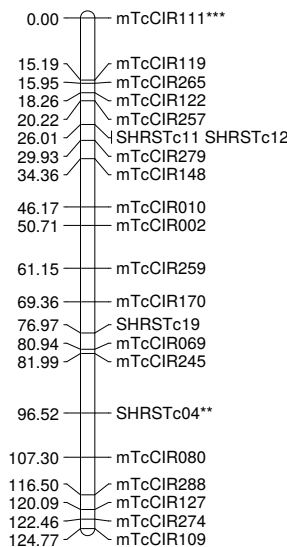
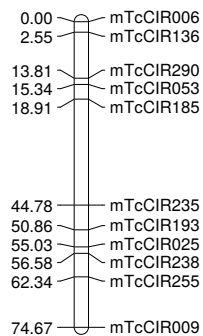
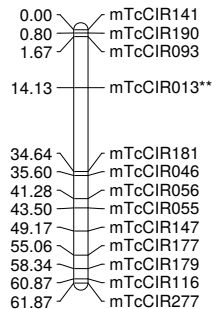
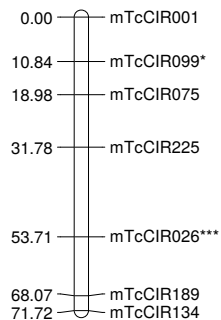
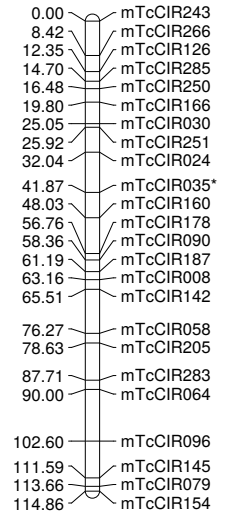
**Figure 2. Physical “*in silico*” map constructed for the cacao tree (*Theobroma cacao* L.) using the sequence of the polymorphic markers detected for the 265 individuals of an F1 segregating population (TSH 1188 X CCN 51).**

This map consists of 217 SSRs covering more than 200 Mb (202.74 Mb) of the available cacao genome. The asterisks shown at the end of the name of some markers represent the following: \*, deviation of segregation (ds); \*\*, not aligned in the multipoint genetic linkage map; \*\*\*, not aligned in the same linkage group of the multipoint genetic map; \*\*\*\*, (ds) and not aligned in the multipoint genetic map; and \*\*\*\*\*, (ds) and not aligned in the same linkage group of the multipoint genetic map. IP and FP represent the initial and final positions of the chromosomes, respectively, obtained from the available cacao genome.

**Figure 3. QTL mapping for the cacao tree (*Theobroma cacao* L.) associated with resistance to black pod disease resulting from infections with *P. palmivora*, *P. citrophthora* and *P. capsici*.**

The LOD score-based thresholds obtained from 1,000 permutation tests are plotted and are based on the method of Chen and Storey (2006) (thick dotted lines).



**LG1****LG2****LG3****LG4****LG5****LG6****LG7****LG8****LG9****LG10**